Supporting Information for:

Terminal Phosphinidene Formation via Tantalaziridine Complexes

Matthew A. Rankin[‡†] and Christopher C. Cummins[‡]*

[‡]*Department of Chemistry, Room 6-435, Massachusetts Institute of Technology*
77 Massachusetts Avenue, Cambridge, MA, USA, 02139-4307

[†]*Current Address: 3M Canada Company, 1360 California Avenue, Box 665,*
Brockville, ON, Canada, K6V 5V8

Email: ccummins@mit.edu

Contents:

SI. Experimental Details

General Considerations. All manipulations were either performed using standard Schlenk methods or in a Vacuum Atmospheres model MO-40M glove box under an atmosphere of purified dinitrogen. Solvents were obtained anhydrous and oxygen-free from a Contour Glass Solvent Purification System. Chloroform was dried and degassed by storing over CaH_2 for 7 d, followed by vacuum distillation. After purification, all solvents were stored under an atmosphere of dinitrogen over 4 Å molecular sieves. Deuterated solvents for NMR spectroscopy were purchased from Cambridge Isotope Laboratories, degassed, and stored over 4 Å molecular sieves for at least 3 d prior to use. Celite 435 (EM Science) and 4 Å molecular sieves (Aldrich) were dried by heating at 200 °C under dynamic vacuum for at least 24 h prior to use. Lithiated phosphanides $LiPPh_2$, LiP(H)Ph, and LiP(H)Cy were prepared via treatment of cold (–35 °C) hexane solutions of the respective phosphine with *n*-BuLi (1.6 M in hexane). Precipitated solids were then collected on a frit after 1 h, washed liberally with hexane, and dried *in vacuo*. Compounds $(Ar[CMe_3CH_2]N)_3TaI_2$ (Ar = 3,5-$Me_2C_6H_3$),[1] $(Ar[CMe_3CH_2]N)_2(\eta^2\text{-}Me_3CC(H)NAr)TaH$ (**2**),[1] and KCH_2Ph[2] were prepared according to previously reported procedures. Otherwise, reagents were obtained from commercial sources and were used as received. All sintered glass frits used were of medium porosity. Unless otherwise indicated, all manipulations were carried out at room temperature (20 °C). During storage for extended periods of time (*ca.* > 3 d), the isolated complexes described herein were typically placed in the glovebox freezer (–35 °C). Elemental analyses were performed by Midwest Microlab (Indianapolis, IN, USA). Unless otherwise stated, NMR characterization data were collected at 20 °C on Bruker AVANCE-400 spectrometers (equipped with either Magnex Scientific or SpectroSpin superconducting magnets) operating at 400.13 (^{1}H), 161.97 (^{31}P), and 100.62 (^{13}C) MHz with chemical shifts reported in parts per million downfield of $SiMe_4$ for ^{1}H and ^{13}C. ^{31}P NMR spectra were referenced externally to 85% H_3PO_4 (0 ppm). ^{1}H and $^{13}C\{^1H\}$ NMR spectra were referenced internally using residual protio-solvent signals.[3] ^{1}H and $^{13}C\{^1H\}$ NMR chemical shift assignments are given on the basis of data obtained from ^{13}C–DEPT, ^{1}H–^{1}H COSY, ^{1}H–^{13}C HSQC, and ^{1}H–^{13}C HMBC NMR experiments. IR spectra were obtained on a Perkin-Elmer Model 2000 FT-IR spectrophotometer.

Synthesis of $(Ar[CMe_3CH_2]N)_3TaPPh$ (1) from $(Ar[CMe_3CH_2]N)_3TaI_2$ and LiP(H)Ph. To a glass vial containing a thawing, bright yellow, magnetically stirred suspension of $(Ar[CMe_3CH_2]N)_3TaI_2$ (0.890 g, 0.882 mmol) in Et_2O (10 mL) was added solid LiP(H)Ph (0.215 g, 1.85 mmol, 2.1 equiv) in small portions over the course of several minutes. The color of the mixture gradually darkened to orange and then to deep red within 45 min. After 17 h, the mixture was dark red-brown and a fine grey precipitate was noticed. NMR spectroscopic analysis of a dried aliquot of the reaction mixture (in 0.8 mL C_6D_6) taken after this time period revealed the presence of **1** and unligated $Ar[CMe_3CH_2]NH$[4] in a *ca.* 3:1 ratio. ^{31}P NMR analysis indicated the presence of the expected byproduct H_2PPh along with several unidentified P-containing species. All volatile materials were then removed from the reaction mixture *in vacuo*, and the residue was extracted twice with *n*-pentane (7 mL) in an effort

to remove residual LiI. After the removal of volatiles under reduced pressure, the remaining solid was treated with a minimum amount of *n*-pentane sufficient for its dissolution (*ca.* 4 mL) and the mixture was placed in the glovebox freezer at −35 °C. After 3 d, a dark red microcrystalline solid was isolated by decantation of the supernatant solution. The solid was then washed quickly with a small amount of thawing *n*-pentane (0.5 mL). The remaining solid was dried *in vacuo*, which left **1** as a spectroscopically pure (see below for spectroscopic details), dark red powder (0.168 g, 0.144 mmol, 19% yield).

Treatment of (Ar[CMe$_3$CH$_2$]N)$_2$(η^2-Me$_3$C*C*(H)*N*Ar)TaH (2) with PhPH$_2$. To a vial containing a solution of **2** (0.103 g, 0.137 mmol) in C_6D_6 (1 mL) was added $PhPH_2$ (0.015 mL, 0.137 mmol) via microsyringe. The resulting mixture was then transferred to an NMR tube. After 3 h, the color of the solution had darkened slightly from yellow to brown-yellow. After this time period, several species were tentatively identified in the reaction mixture by ^{1}H (400.1 MHz, 20 °C) and ^{31}P (162.0 MHz, 20 °C) NMR spectroscopy by comparison to a previously reported reaction that followed a similar course,[5a] including the addition product (Ar[CMe$_3$CH$_2$]N)$_3$Ta(H)P(H)Ph (*diagnostic features*[5a,b] *include*: ^{31}P NMR: δ 9.9 (dd, $^1J_{PH}$ = 207 Hz, $^2J_{PH}$ = 64 Hz), ^{1}H NMR: δ 23.59 (dd, $^2J_{HP}$ = 64 Hz, $^3J_{HH}$ = 2.5 Hz, Ta(*H*)P(H)Ph), 5.88 (dd, $^1J_{HP}$ = 207 Hz, $^3J_{HH}$ = 2.5 Hz, Ta(H)P(*H*)Ph)), the dihydride (Ar[CMe$_3$CH$_2$]N)$_3$Ta(H)$_2$ (*diagnostic features*[5c] *include*: ^{1}H NMR: δ 20.65 (s, Ta(*H*)$_2$)), as well as (Ar[CMe$_3$CH$_2$]N)$_3$TaPPh (**1**), [(Ar[CMe$_3$CH$_2$]N)$_3$Ta(μ-H)]$_2$ (**8**), and (Ar[CMe$_3$CH$_2$]N)$_2$(η^2-Me$_3$C*C*(H)*N*Ar)TaP(H)Ph (**3**), the latter three being complexes that are characterized fully herein (*vide infra*). In addition, unconsumed $PhPH_2$ along with the starting hydride **2** and its ring-expanded isomer[1] (Ar[CMe$_3$CH$_2$]N)$_2$(κ^2-*C*H$_2$C(Me)$_2$CH$_2$*N*Ar)TaH were also observed. Given the complexity of the reaction mixture, we are hesitant to comment definitively regarding the reaction pathway and the relative amounts of each constituent. After 3 d, the contents of the mixture had become less complicated, with only **1** (*ca.* 22% yield by integration versus an internal $Me_3SiOSiMe_3$ standard), **2** (and its ring-expanded isomer), and unreacted $PhPH_2$ present, as observed by NMR spectroscopy. Deep red crystals present within the NMR tube after 3 d were identified as **8** by X-ray crystallography (*vide infra*). In an attempt to circumvent the competitive consumption of **2** by the apparent reaction with side-product H_2, an analogous reaction to that reported above was conducted under static vacuum. Although the yield of **1** was slightly increased (*in situ*) and the formation of **8** was less evident, the reaction likewise did not proceed to completion, as unreacted **2** (and its ring-expanded isomer) and $PhPH_2$ were detected in comparable amounts after 3 d.

Independent preparation of [(Ar[CMe$_3$CH$_2$]N)$_3$Ta(μ-H)]$_2$ (8) from (Ar[CMe$_3$CH$_2$]N)$_2$(η^2-Me$_3$C*C*(H)*N*Ar)TaH (2) and H$_2$. A 100 mL sealable reaction vessel was charged with a yellow solution of **2** (0.556 g, 0.740 mmol) in C_6H_6 (8 mL). The contents of the vessel were then thoroughly degassed via three freeze-pump-thaw cycles. An atmosphere of H_2 (*ca.* 1 atm) was then introduced into the vessel over the course of several minutes. The vessel was then sealed and the mixture was stirred magnetically. Within 15 min, the solution had gradually darkened in color from yellow to reddish-brown. After 2 h, further darkening of the solution was observed and a fine reddish-brown precipitate was noticed. After 48 h, after which time substantially more solid had precipitated, the volume of the reaction mixture was reduced by *ca.* 1 mL. The mixture was then filtered through a frit, and the collected solids were rinsed with C_6H_6 (10 mL) and *n*-hexane (10 mL). The residual solid was dried under reduced pressure, which left **8** as an analytically pure, fine red-brown powder (0.434 g, 0.289 mmol, 78% yield). When a similar reaction to that reported above was repeated with C_6D_6 as the solvent, the Ta−*H* ^{1}H NMR signal at 20.65 ppm tentatively assigned to the monomeric dihydride (Ar[CMe$_3$CH$_2$]N)$_3$Ta(H)$_2$ (*vide supra*) was observed in the reaction mixture as a minor constituent (along with major components **2** and **8)** after 3 h, but was not evident in the ^{1}H NMR spectrum after 48 h. We therefore postulate that this complex is an intermediate in the formation of **8**. When the above reaction was repeated in the absence of magnetic stirring, deep red hexagonal crystals suitable for X-ray diffraction were deposited from the reaction mixture.[6] Anal. calcd for $C_{78}H_{122}N_6Ta_2$ (FW: 1504.87 g/mol): C 62.20; H 8.17; N 5.58. Found: C 62.45; H 7.89; N 5.62. ^{1}H NMR (THF-d_8, 400.1 MHz, 20 °C): δ 8.78 (s, 2H, [Ta(μ-H)]$_2$), 6.65 (s, 6H, *p*-ArH), 6.16 (s, 12H, *o*-ArH), 4.48 (s, 12H, NCH_2), 2.13 (s, 36H, Ar-*Me*), 0.79 (s, 54H, CMe_3). Despite prolonged acquisition times, the limited solubility of **8** in common organic solvents precluded the acquisition of meaningful data from ^{13}C NMR spectroscopic experiments. An IR spectrum collected on a sample of **8** (thin film, KBr) revealed the absence of an obvious absorbance attributable to a terminal Ta−H moiety (see Figure S-1).[7] Further evidence for a structural formulation containing Ta−H linkages comes from the formation of (Ar[CMe$_3$CH$_2$]N)$_3$TaCl$_2$ (**9**) from the treatment of **8** (0.123 g, 0.0817 mmol) with $CDCl_3$ (0.8 mL). After 0.5 h, the resulting mixture contained only signals attributable to **8**: ^{1}H NMR ($CDCl_3$, 400.1 MHz, 20 °C): δ 8.84 (s, 2H, [Ta(μ-H)]$_2$, 6.70 (s, 6H, *p*-ArH), 6.20 (s, 12H, *o*-ArH), 4.50 (s, 12H, NCH_2), 2.22 (s, 36H, Ar-*Me*), 0.86 (s, 27H, CMe_3). However, after 36 h, no signals corresponding to **8** were

observable by ^{1}H NMR spectroscopy. Instead, a mixture of complexes was observed by ^{1}H NMR spectroscopy, one component being (Ar[CMe_3CH_2]N)$_3$TaCl$_2$ (**9**, *ca.* 32%). The net hydride/halogen exchange evident in the production of **9** is consistent with previous studies of Ta−H complexes.[6b,c] Yellow crystals of **9** suitable for a X-ray diffraction were grown via slow evaporation of the NMR tube contents (see Figure S-10).[8] NMR spectroscopic data obtained upon dissolution of these crystals in C_6D_6 compared favorably to published data for **9**.[9]

Synthesis of (Ar[CMe_3CH_2]N)$_2$(η^2-Me_3CC(H)*N*Ar)TaCl (4). To a glass vial containing (Ar[CMe_3CH_2]N)$_2$(η^2-Me_3CC(H)*N*Ar)TaH (**2**, 0.428 g, 0.570 mmol) was added $CHCl_3$ (6 mL). The resulting solution was stirred magnetically for 24 h. After this time period, an aliquot of the reaction mixture was transferred to a vial, dried *in vacuo*, and treated with C_6D_6 (0.5 mL). NMR spectroscopic analysis of this solution showed the complete disappearance of the Ta-*H* signal associated with **2** and quantitative formation of a new tantalaziridine complex, subsequently identified as **4**. The NMR tube contents were then combined with the original vial contents and the mixture was dried *in vacuo*. The residual oily yellow solid was triturated with *n*-pentane (2 × 4 mL) and then dried under reduced pressure, which left **4** as an analytically pure, yellow powder (0.430 g, 0.547 mmol, 96% yield). A crystal suitable for X-ray diffraction was grown from a solution of **4** in Et_2O stored at −35 °C.[10] Equivalent phenyl resonances in the ^{1}H and ^{13}C NMR spectra indicated free rotation of the P−C and Ta−P bonds in C_6D_6 solution. Anal. calcd for $C_{39}H_{59}N_3ClTa$ (785.87 g/mol): C 59.55; H 7.57; N 5.35. Found: C 59.24; H 7.51; N 5.07. ^{1}H NMR (C_6D_6, 400.1 MHz, 20 °C): δ 7.50 (br s, 2H, *o*-Ar), 6.79 (s, 2H, *o*-Ar), 6.60 (s, 1H, *p*-Ar), 6.55-6.53 (m, 2H, 2 *p*-Ar), 6.41 (br s, 2H, *o*-Ar), 4.63-4.54 (AB m, 2H, NCH_aH_b), 3.17 (d, $^2J_{HH}$ = 14.0 Hz, 1H, NCH_cH$_d$), 3.02 (d, $^2J_{HH}$ = 14.0 Hz, 1H, NCH$_c$$H_d$), 2.32 (s, 6H, Ar-*Me*), 2.29 (s, 1H, NC(*H*)CMe_3), 2.19 (s, 6H, Ar-*Me*), 2.03 (s, 6H, Ar-*Me*), 1.14 (s, 9H, NC(H)CMe_3), 0.81 (s, 9H, CH_2CMe_3), 0.51 (s, 9H, CH_2CMe_3); ^{13}C NMR (C_6D_6, 100.6 MHz, 20 °C): δ 155.7 (aziridine NAr *ipso*), 146.1 (NAr *ipso*), 140.5 (*m*-Ar), 139.4 (*m*-Ar), 138.9 (NAr *ipso*), 138.1 (*m*-Ar), 128.5 (*p*-Ar), 128.3 (*p*-Ar), 124.9 (br, *o*-Ar), 124.4 (br, *o*-Ar), 123.2 (*p*-Ar), 117.8 (*o*-Ar), 91.7 (N*C*(H)CMe_3), 70.5 (N*C*H$_a$H$_b$), 65.6 (NCH$_c$H$_d$), 37.8 (NC(H)*C*Me$_3$), 36.4 (CH_2CMe_3), 35.8 (CH_2CMe_3), 32.7 (NC(H)CMe_3), 29.5 (CH_2CMe_3), 28.7 (CH_2CMe_3), 22.3 (Ar-*Me*), 21.8 (Ar-*Me*), 21.5 (Ar-*Me*).

Synthesis of (Ar[CMe_3CH_2]N)$_2$(η^2-Me_3CC(H)*N*Ar)TaPPh$_2$ (5). To a glass vial containing solid $LiPPh_2$ (0.048 g, 0.252 mmol) was added a mixture of (Ar[CMe_3CH_2]N)$_2$(η^2-Me_3CC(H)*N*Ar)TaCl (**4**, 0.198 g, 0.252 mmol) and C_6H_6 (6 mL) via pipette. After the resulting mixture was stirred magnetically for 2 h, the orange mixture was filtered through a plug of Celite, and the filtrate was dried *in vacuo*. The oily orange residue was then treated with *n*-pentane (6 mL) and the resulting mixture was filtered through a plug of Celite. The filtrate was then stored at −35 °C. After 3 d, an orange microcrystalline solid was isolated by decantation of the supernatant solution. The solid was dried *in vacuo*, which left **5** as an analytically pure, orange powder (0.198 g, 0.212 mmol, 84% yield). A crystal suitable for X-ray diffraction was grown from a solution of **5** in Et_2O stored at −35 °C.[11] Anal. calcd for $C_{51}H_{69}N_3PTa$ (935.47 g/mol): C 65.42; H 7.43; N 4.49. Found: C 65.45; H 7.36; N 4.42. ^{1}H NMR (C_6D_6, 400.1 MHz, 20 °C): δ 7.30-7.24 (m, 4H, PAr), 7.20-7.15 (m, 4H, PAr), 7.09 (br s, 2H, *o*-Ar), 7.04-7.01 (m, 2H, PAr), 6.96 (s, 2H, *o*-Ar or 2 *p*-Ar), 6.68 (s, 1H, *p*-Ar), 6.54 (s, 2H, 2 *p*-Ar or *o*-Ar), 6.07 (br s, 2H, *o*-Ar), 4.43 (d, $^2J_{HH}$ = 14.0 Hz, 1H, NCH_aH$_b$), 4.30 (d, $^2J_{HH}$ = 14.0 Hz, 1H, NCH$_a$$H_b$), 3.60 (d, $^2J_{HH}$ = 14.0 Hz, 1H, NCH_cH$_d$), 3.49 (d, $^2J_{HH}$ = 14.0 Hz, 1H, NCH$_c$$H_d$), 3.46 (m, 1H, NC(*H*)$CMe_3$), 2.28 (s, 6H, Ar-*Me*), 2.20 (s, 6H, Ar-*Me*), 2.00 (s, 6H, Ar-*Me*), 1.30 (s, 9H, NC(H)CMe_3), 0.90 (s, 9H, CH_2CMe_3), 0.50 (s, 9H, CH_2CMe_3); ^{13}C NMR (C_6D_6, 100.6 MHz, 20 °C): δ 157.1 (aziridine NAr *ipso*), 147.6 (NAr *ipso*), 145.7 (PAr *ipso*), 145.2 (NAr *ipso*), 139.4 (*m*-Ar), 138.9 (*m*-Ar), 138.2 (*m*-Ar), 135.5 (d, J_{PC} = 13.1 Hz, 2 PAr), 128.5 (d, J_{PC} = 8.0 Hz, 2 PAr), 127.8 (*p*-Ar), 127.5 (*p*-Ar), 127.2 (PAr), 125.5 (*o*-Ar), 123.6 (*p*-Ar), 123.1 (br, *o*-Ar), 118.5 (br, *o*-Ar), 85.1 (d, $^2J_{PC}$ = 12.5 Hz, N*C*(H)CMe_3), 69.5 (d, $^3J_{PC}$ = 15.5 Hz, N*C*H$_a$H$_b$), 64.0 (N*C*H$_c$H$_d$), 39.1 (NC(H)*C*Me$_3$), 36.5 (CH_2CMe_3), 34.7 (CH_2CMe_3), 33.5 (d, $^4J_{PC}$ = 2.2 Hz, NC(H)CMe_3), 30.0 (CH_2CMe_3), 29.1 (CH_2CMe_3), 22.1 (Ar-*Me*), 22.0 (Ar-*Me*), 21.7 (Ar-*Me*); ^{31}P{^{1}H} NMR (C_6D_6, 162.0 MHz, 20 °C): δ 112.0.

Synthesis of (Ar[CMe_3CH_2]N)$_2$(η^2-Me_3CC(H)*N*Ar)TaP(H)Ph (3). To a glass vial containing solid LiP(H)Ph (0.105 g, 0.908 mmol, 3 equiv) was added a mixture of (Ar[CMe_3CH_2]N)$_2$(η^2-Me_3CC(H)*N*Ar)TaCl (**4**, 0.238 g, 0.303 mmol) and C_6H_6 (6 mL) via pipette. After the resulting mixture was stirred magnetically for 1 h, the dark yellow-orange mixture was filtered through a plug of Celite. ^{31}P NMR spectroscopic analysis of an aliquot of the reaction mixture revealed the presence of **3** and (Ar[CMe_3CH_2]N)$_3$TaPPh (**1**) in a *ca.* 15:1 ratio. (*Note:* It was observed that the addition of < 3 equivalents (1-1.5) of LiP(H)Ph to **4** led to reaction mixtures containing the desired product **3** in lower proportions as compared to **4** (at shorter reaction times, e.g. < 1 h) or **1** (at longer reaction times, e.g. 3-24 h)). After the filtrate was dried *in vacuo*, the oily orange residue was then treated with *n*-pentane (6 mL) and the resulting mixture was filtered through a plug of Celite. The filtrate was then stored at −35

^{o}C. After 3 d, a yellow-orange microcrystalline solid was isolated by decantation of the supernatant solution. The spectroscopically pure solid was dried *in vacuo*, providing **3** as an analytically pure, yellow-orange powder (0.120 g, 0.139 mmol, 46% yield). A crystal suitable for X-ray diffraction was grown from a solution of **3** in *n*-pentane stored at −35 ^{o}C.[12] Anal. calcd for $C_{45}H_{65}N_3PTa$ (FW: 859.44 g/mol): C 62.83; H 7.62; N 4.89. Found: C 62.71; H 7.51; N 4.60. ^{1}H NMR (C_6D_6, 400.1 MHz, 20 ^{o}C): δ 7.65 (m, 2H, PAr), 7.21 (m, 2H, PAr), 7.07 (s, 2H, Ar), 7.02 (s, 1H, PAr), 6.81 (s, 2H, Ar), 6.59 (s, 2H, Ar), 6.53 (apparent s, 3H, Ar), 5.39 (d, $^{1}J_{PH}$ = 229 Hz, 1H, PH), 4.07 (d, $^{2}J_{HH}$ = 14.0 Hz, 1H, NCH_aH$_b$), 3.93 (d, $^{2}J_{HH}$ = 14.0 Hz, 1H, NCH$_a$$H_b$), 3.04-2.92 (AB m, 2H, NC$H_c$$H_d$), 2.32 (s, 6H, Ar-*Me*), 2.24 (s, 1H, NC(*H*)CMe$_3$), 2.08 (s, 6H, Ar-*Me*), 2.02 (s, 6H, Ar-*Me*), 1.43 (s, 9H, NC(H)C*Me*$_3$), 0.76 (s, 9H, CH$_2$C*Me*$_3$), 0.44 (s, 9H, CH$_2$C*Me*$_3$); ^{13}C NMR (C_6D_6, 100.6 MHz, 20 ^{o}C): δ 156.5 (aziridine NAr *ipso*), 146.2 (NAr *ipso*), 146.1 (NAr *ipso*), 145.6 (d, $^{1}J_{PC}$ = 24.7 Hz, PAr *ipso*), 139.7 (*m*-Ar), 139.0 (*m*-Ar), 138.2 (*m*-Ar), 133.9 (d, J_{PC} = 13.3 Hz, 2 PAr), 127.9-127.5 (m, 3 PAr and *o*-Ar), 125.9 (*p*-Ar), 124.5 (br, *o*-Ar), 123.6 (*p*-Ar), 122.9 (*p*-Ar), 117.2 (*o*-Ar), 87.4 (d, $^{2}J_{PC}$ = 3.4 Hz, N*C*(H)CMe$_3$), 66.8 (d, $^{3}J_{PC}$ = 2.1 Hz, N*C*H$_a$H$_b$), 62.1 (d, $^{3}J_{PC}$ = 3.3 Hz, N*C*H$_c$H$_d$), 39.4 (NC(H)*C*Me$_3$), 36.0 (CH$_2$*C*Me$_3$), 35.2 (CH$_2$*C*Me$_3$), 33.4 (d, $^{4}J_{PC}$ = 4.7 Hz, NC(H)C*Me*$_3$), 29.3 (CH$_2$C*Me*$_3$), 29.1 (CH$_2$C*Me*$_3$), 22.2 (Ar-*Me*), 21.8 (Ar-*Me*), 21.7 (Ar-*Me*); ^{31}P NMR (C_6D_6, 162.0 MHz, 20 ^{o}C): δ −19.1 (d, $^{1}J_{PH}$ = 229 Hz).

Synthesis of (Ar[CMe$_3$CH$_2$]N)$_3$TaPPh (1) from (Ar[CMe$_3$CH$_2$]N)$_2$(η^2-Me$_3$C*C*(H)*N*Ar)TaCl (4) and LiP(H)Ph. To a vial containing a suspension of LiP(H)Ph (0.094 g, 0.813 mmol, 1.5 equiv) in C_6H_6 (5 mL) was added dropwise a yellow mixture of (Ar[CMe$_3$CH$_2$]N)$_2$(η^2-Me$_3$C*C*(H)*N*Ar)TaCl (**4**, 0.426 g, 0.542 mmol) and C_6H_6 (5 mL). After the mixture was stirred magnetically for 24 h, the coloration of the mixture had become deep red. NMR spectroscopic analysis of this solution showed quantitative formation of **1** (see Figure S4 for further details). After this time period, the mixture was filtered through a plug of Celite, and the filtrate was dried under reduced pressure. The oily dark red residue was triturated with *n*-pentane (2 × 5 mL) and was then treated with *n*-pentane (6 mL), followed by filtration of the resulting mixture through a plug of Celite. The filtrate was then dried *in vacuo*, which left **1** as an analytically pure, dark red powder (0.377 g, 0.439 mmol, 81% yield). A crystal suitable for X-ray diffraction was grown from a solution of **1** in *n*-pentane stored at −35 ^{o}C. Anal. calcd for $C_{45}H_{65}N_3PTa$ (FW: 859.44 g/mol): C 62.83; H 7.62; N 4.89. Found: C 62.54; H 7.47; N 4.68. ^{1}H NMR (C_6D_6, 400.1 MHz, 20 ^{o}C): δ 7.77 (d, *J* = 6.8 Hz, 2H, PAr), 7.31 (apparent t, *J* = 7.4 Hz, 2H, PAr), 6.86 (m, 1H, PAr), 6.58 (s, 6H, *o*-Ar), 6.54 (s, 3H, *p*-Ar), 4.43 (s, 6H, NCH$_2$), 2.07 (s, 18H, Ar-*Me*), 0.92 (s, 27H, CMe$_3$); ^{13}C{^{1}H} NMR (C_6D_6, 100.6 MHz, 20 ^{o}C): δ 150.5 (NAr *ipso*), 139.0 (*m*-Ar), 135.4 (2 PAr), 133.9 (d, $^{1}J_{PC}$ = 13.4 Hz, PAr *ipso*), 128.2 (2 PAr), 126.6 (*p*-Ar), 126.5 (PAr), 122.9 (*o*-Ar), 76.5 (d, $^{3}J_{PC}$ = 7.8 Hz, NCH$_2$), 36.2 (*C*Me$_3$), 29.8 (C*Me*$_3$), 21.9 (Ar-*Me*); ^{31}P{^{1}H} NMR (C_6D_6, 162.0 MHz, 20 ^{o}C): δ 451.6.

Synthesis of (Ar[CMe$_3$CH$_2$]N)$_3$TaPCy (6). To a vial containing a suspension of LiP(H)Cy (0.079 g, 0.650 mmol, 1.5 equiv) in C_6H_6 (5 mL) was added dropwise a yellow solution of (Ar[CMe$_3$CH$_2$]N)$_2$(η^2-Me$_3$C*C*(H)*N*Ar)TaCl (**4**, 0.340 g, 0.433 mmol) in C_6H_6 (5 mL). After the mixture was stirred magnetically for 18 h, the coloration of the mixture had become deep red. After this time period, the mixture was filtered through a plug of Celite, and the filtrate was dried under reduced pressure. The oily dark red residue was triturated with *n*-pentane (2 × 5 mL) and was then treated with *n*-pentane (6 mL), followed by filtration of the resulting mixture through a plug of Celite. The filtrate was then dried *in vacuo*, which left **6** as an analytically pure, brownish-red powder (0.322 g, 0.372 mmol, 86% yield). A crystal suitable for X-ray diffraction was grown from a solution of **6** in a Et$_2$O/ *n*-pentane mixture (*ca.* 1:1) stored at −35 ^{o}C. Anal. calcd for $C_{45}H_{71}N_3PTa$ (FW: 865.48 g/mol): C 62.39; H 8.27; N 4.85. Found: C 62.04; H 8.07; N 4.94. ^{1}H NMR (C_6D_6, 400 MHz, 20 ^{o}C): δ 6.59 (s, 6H, *o*-ArH), 6.54 (s, 3H, *p*-ArH), 5.07 (br s, 1H, P-C(H)), 4.47 (s, 6H, NCH$_2$), 2.47 (apparent br d, *J* = 11.2 Hz, 2H, Cy-H), 2.11 (s, 18H, Ar-*Me*), 1.88-1.83 (m, 2H, Cy-H), 1.63-1.48 (m, 5H, Cy-H), 1.26 (m, 1H, Cy-H), 1.05 (s, 27H, CMe$_3$); ^{13}C NMR (C_6D_6, 100.6 MHz, 20 ^{o}C): δ 151.2 (NAr *ipso*), 139.0 (*m*-Ar), 126.2 (*p*-Ar), 122.3 (*o*-Ar), 78.6 (NCH$_2$), 49.8 (d, $^{1}J_{CP}$ = 42.4 Hz, P-C(H)), 39.1 (Cy CH$_2$), 36.0 (*C*Me$_3$), 29.9 (C*Me*$_3$), 28.3 (Cy CH$_2$), 26.9 (Cy CH$_2$), 21.9 (Ar-*Me*); ^{31}P{^{1}H} NMR (C_6D_6, 162.0 MHz, 20 ^{o}C): δ 483.1.

Formation of PhP=C(H)^{t}Bu from the treatment of (Ar[CMe$_3$CH$_2$]N)$_3$TaPPh (1) with O=C(H)^{t}Bu. To a vial containing a solution of **1** (0.103 g, 0.120 mmol) in C_6D_6 (1 mL) was added O=C(H)^{t}Bu (0.016 mL, 0.144 mmol, 1.2 equiv) via microsyringe. Upon addition of the aldehyde, the color of the solution was observed to change from deep red to pale yellow within 10 min. The contents of the vial were then transferred to an NMR tube. After 30 min, ^{31}P NMR spectroscopy indicated the complete consumption of **1** and conversion to a single P-containing species that corresponds to a new singlet at 224.3 ppm. Quantification of the contents of the reaction mixture by ^{1}H NMR spectroscopy (using Me$_3$SiOSiMe$_3$ as an internal standard) showed that PhP=C(H)^{t}Bu was produced in >95% yield.

Identification of PhP=C(H)^{t}Bu was made by comparison to previously published data available for this compound.[13] No efforts were made toward the purification of PhP=C(H)^{t}Bu from the reaction mixture. As of yet, we have not been able to ascertain the fate of the tantalum-containing byproduct(s).

Formation of CyP=C(H)^{t}Bu from the treatment of (Ar[CMe$_3$CH$_2$]N)$_3$TaPCy (6) with O=C(H)^{t}Bu. An analogous procedure to that used above for the formation of PhP=C(H)^{t}Bu was followed, with the exception that **6** was used in place of (Ar[CMe$_3$CH$_2$]N)$_3$TaPPh (**1**). The *in situ* yield for the formation of the phosphaalkene was >95% (^{1}H NMR, Me$_3$SiOSiMe$_3$ as internal standard). Identification of CyP=C(H)^{t}Bu was made by comparison to previously published data available for this compound.[14]

Attempt to prepare (Ar[CMe$_3$CH$_2$]N)$_3$Ta=C(H)Ph: Synthesis of (Ar[CMe$_3$CH$_2$]N)$_2$(η^2-Me$_3$C*C*(H)*N*Ar)TaCH$_2$Ph and spectroscopic observation at 65 ^{o}C. To a vial containing solid KCH$_2$Ph (0.040 g, 0.310 mmol, 1.2 equiv) was added a thawing mixture of (Ar[CMe$_3$CH$_2$]N)$_2$(η^2-Me$_3$C*C*(H)*N*Ar)TaCl (0.203 g, 0.258 mmol) in C$_6$H$_6$ (5 mL). The mixture was then stirred magnetically. Over the course of 20 min, the color of the solution gradually turned dark yellow, and a dark precipitate was observed. After 1 h, the mixture was filtered through a plug of Celite and the filtrate was dried *in vacuo*. The residual solid was triturated with *n*-pentane (2 × 2 mL), and was dried *in vacuo*, which left (Ar[CMe$_3$CH$_2$]N)$_2$(η^2-Me$_3$C*C*(H)*N*Ar)TaCH$_2$Ph as an analytically pure, yellow solid (0.178 g, 0.211 mmol, 82% yield). Anal. calcd for C$_{46}$H$_{66}$N$_3$Ta (841.47 g/mol): C 65.60; H 7.90; N 4.99. Found: C 65.93; H 8.05; N 5.07. ^{1}H NMR (C$_6$D$_6$, 400.1 MHz, 20 ^{o}C): δ 7.43 (m, 2H, CH$_2$*Ph*), 7.34 (m, 2H, CH$_2$*Ph*), 7.20 (s, 2H, *o*-Ar), 7.02 (m, 1H, CH$_2$*Ph*), 6.78 (s, 2H, *o*-Ar), 6.60 (s, 1H, *p*-Ar), 6.52 (s, 1H, *p*-Ar), 6.50-6.45 (m, 3H, *p*-Ar and *o*-Ar), 4.11-3.97 (AB m, 2H, NC*H*$_a$*H*$_b$), 3.74 (d, $^2J_{HH}$ = 14.0 Hz, 1H, NC*H*$_c$H$_d$), 3.05 (d, $^2J_{HH}$ = 14.0 Hz, 1H, NCH$_c$*H*$_d$), 2.94-2.84 (AB m, 2H, C*H*$_a$*H*$_b$Ph), 2.71 (s, 1H, NC(*H*)CMe$_3$), 2.39 (s, 6H, Ar-*Me*), 2.08 (s, 6H, Ar-*Me*), 2.04 (s, 6H, Ar-*Me*), 1.30 (s, 9H, NC(H)C*Me*$_3$), 0.75 (s, 9H, CH$_2$C*Me*$_3$), 0.42 (s, 9H, CH$_2$C*Me*$_3$); ^{13}C NMR (C$_6$D$_6$, 100.6 MHz, 20 ^{o}C): δ 157.1 (aziridine NAr *ipso*), 150.8 (NAr *ipso*), 147.3 (NAr *ipso*), 145.3 (CH$_2$Ph *ipso*), 139.7 (*m*-Ar), 139.0 (*m*-Ar), 138.3 (*m*-Ar), 129.4 (2 CH$_2$*Ph*), 128.7 (2 CH$_2$*Ph*), 128.0 (CH$_2$*Ph*), 127.9 (*p*-Ar), 124.2 (br, *o*-Ar), 123.6-123.4 (m, *p*-Ar and *o*-Ar), 122.8 (*p*-Ar), 117.6 (*o*-Ar), 88.9 (N*C*(H)CMe$_3$), 67.2 (N*C*H$_a$H$_b$), 64.5 (*C*H$_2$Ph), 61.0 (N*C*H$_c$H$_d$), 38.6 (NC(H)*C*Me$_3$), 35.9 (CH$_2$*C*Me$_3$), 34.9 (CH$_2$*C*Me$_3$), 33.2 (NC(H)C*Me*$_3$), 29.4 (CH$_2$C*Me*$_3$), 29.0 (CH$_2$C*Me*$_3$), 22.3 (Ar-*Me*), 22.0 (Ar-*Me*), 21.8 (Ar-*Me*). When a sample of (Ar[CMe$_3$CH$_2$]N)$_2$(η^2-Me$_3$C*C*(H)*N*Ar)TaCH$_2$Ph (0.060 g) was placed in a sealable NMR tube, dissolved in C$_6$D$_6$ (0.8 mL), and was heated at 65 ^{o}C for 12 h, no change in the spectrum was observed by ^{1}H NMR spectroscopy. The impact of the addition of base to solutions of (Ar[CMe$_3$CH$_2$]N)$_2$(η^2-Me$_3$C*C*(H)*N*Ar)TaCH$_2$Ph (beyond the 0.2 equiv excess used in its preparation) has not yet been investigated.

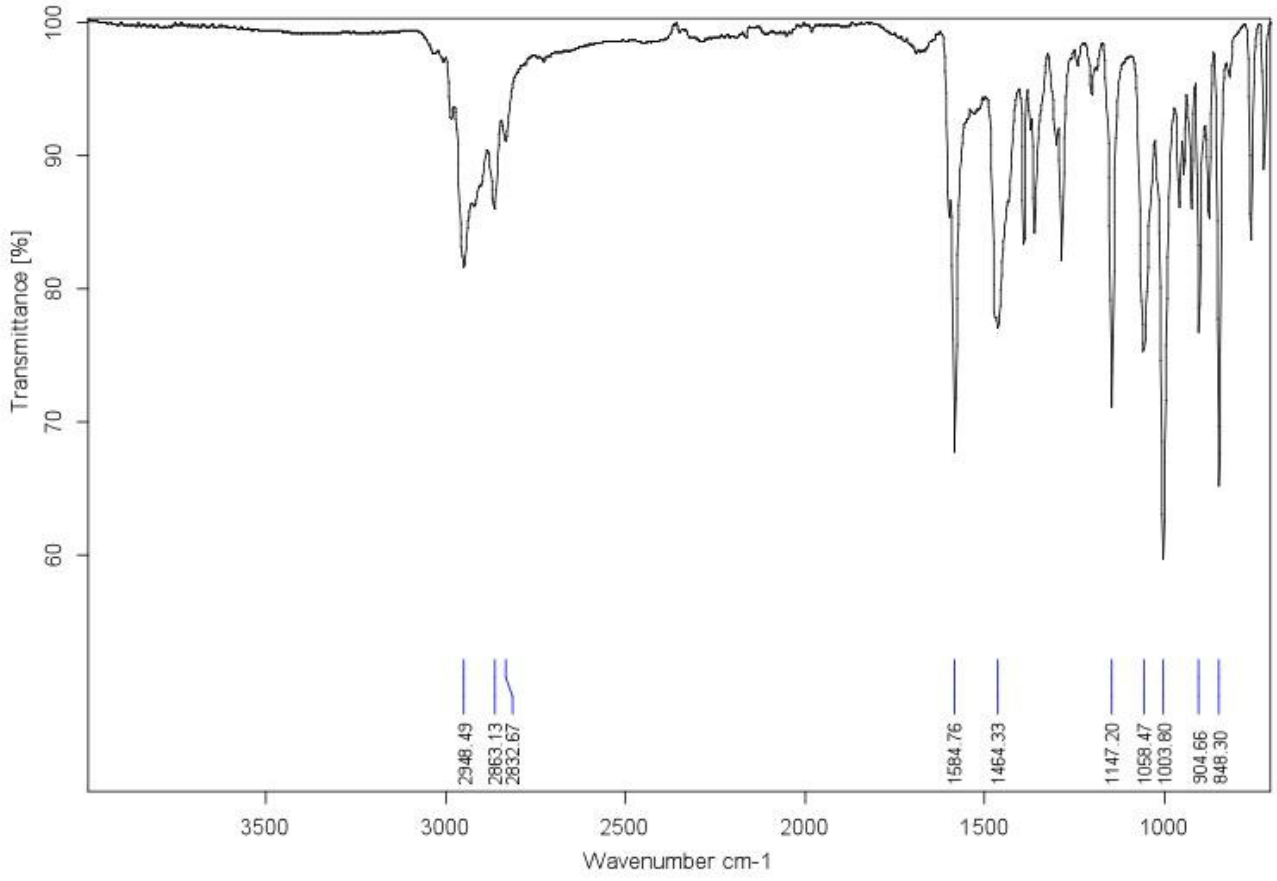

Figure S1. IR Spectrum of $[(Ar[CMe_3CH_2]N)_3Ta(\mu\text{-}H)]_2$ (**8**), thin film (KBr).

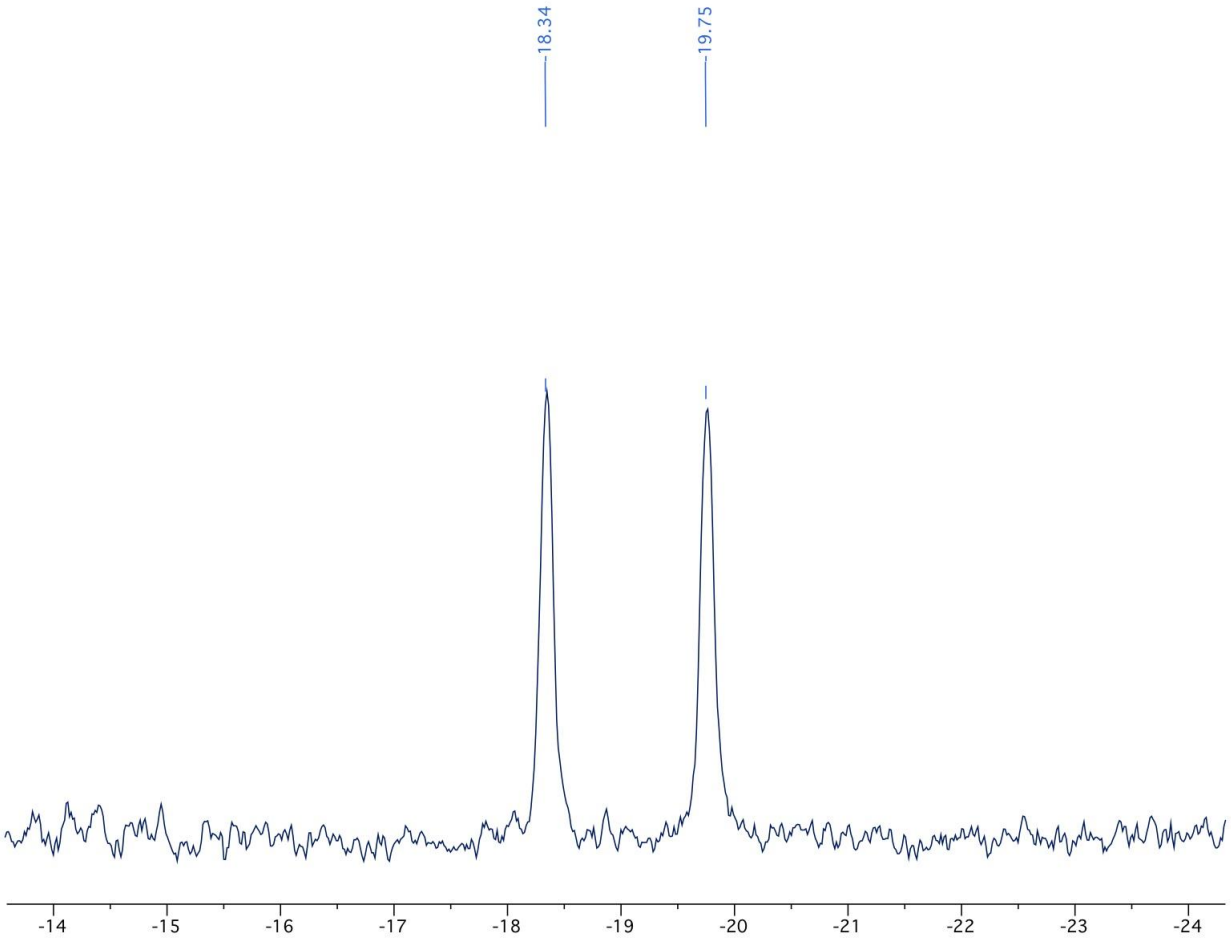

Figure S2. ^{31}P NMR (C_6D_6, 161.97 MHz, 20 ^{o}C) spectrum of (Ar[CMe_3CH_2]N)$_2$(η^2-Me_3CC(H)*N*Ar)TaP(H)Ph (**3**, $^1J_{PH}$ = 229 Hz).

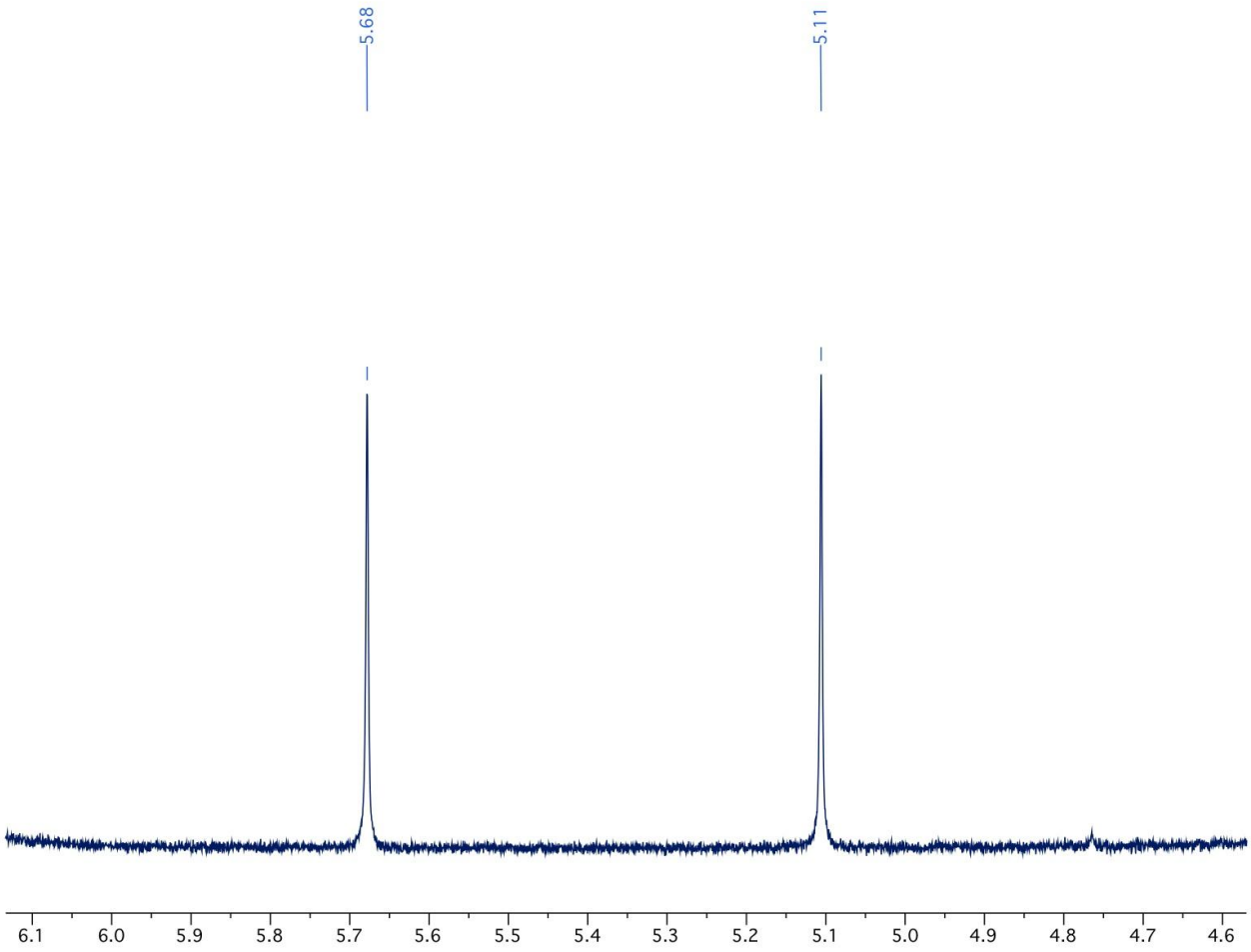

Figure S3. Selected P−*H* region of ^{1}H NMR (C_6D_6, 400.13 MHz, 20 ^{o}C) spectrum of (Ar[CMe_3CH_2]N)$_2$(η^2-Me_3CC(H)*N*Ar)TaP(H)Ph, (**3,** $^{1}J_{HP}$ = 229 Hz).

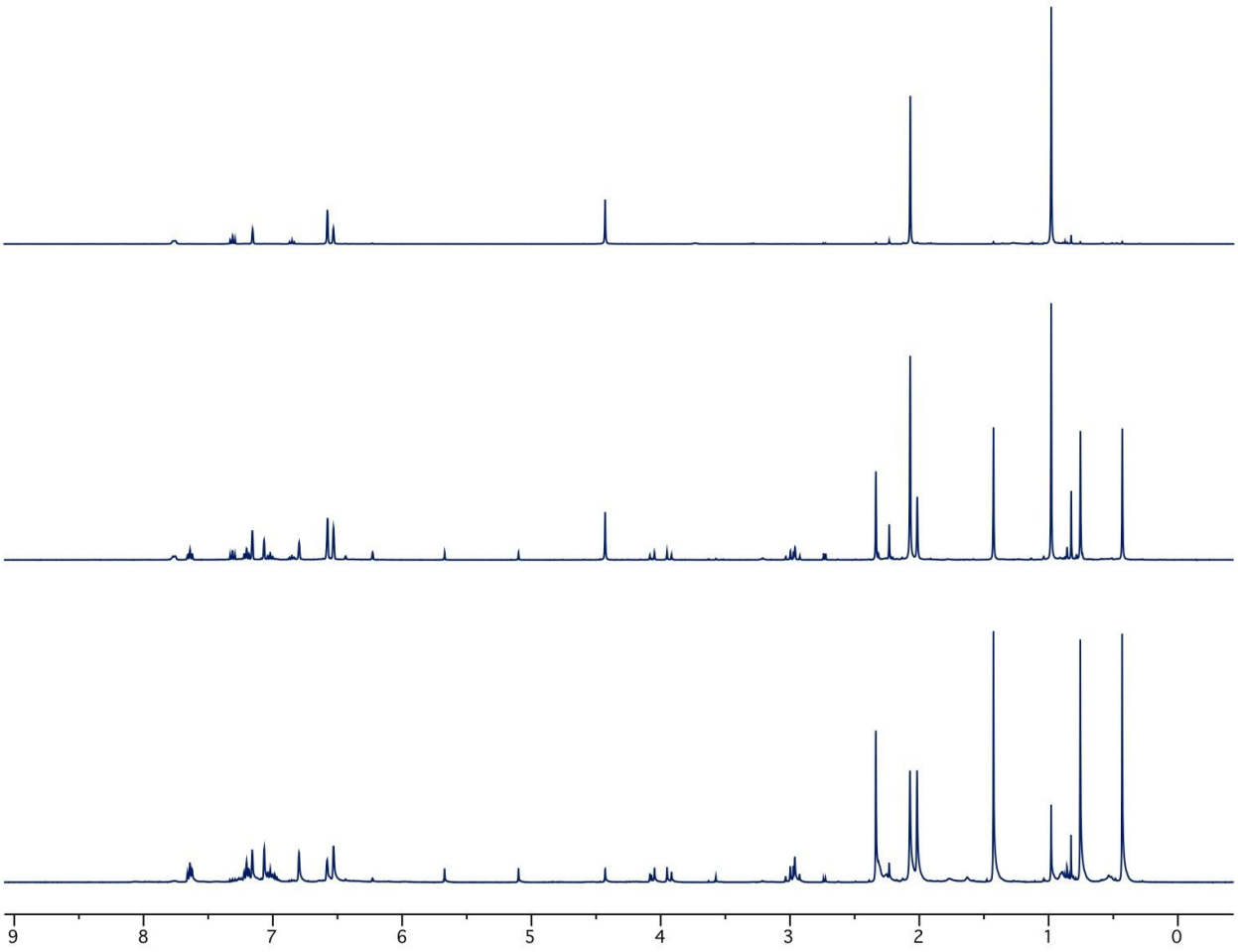

Figure S4. Stack plot of ^{1}H NMR (C_6D_6, 400.13 MHz, 20 ^{o}C) spectra illustrating the course of the reaction *in situ* between (Ar[CMe_3CH_2]N)$_2$(η^2-Me_3C*C*(H)*N*Ar)TaCl (**4**) and 1.5 equiv LiP(H)Ph. *Bottom:* after 60 min. The reaction mixture contains (Ar[CMe_3CH_2]N)$_2$(η^2-Me_3C*C*(H)*N*Ar)TaP(H)Ph (**3**, *ca.* 90%) and (Ar[CMe_3CH_2]N)$_3$TaPPh (**1**, *ca.* 10%); *Middle:* after 4h. The reaction mixture contains **3** (*ca.* 60%) and **1** (*ca.* 40%); *Top:* after 24 h. Reaction mixture contains **1** (>95%).

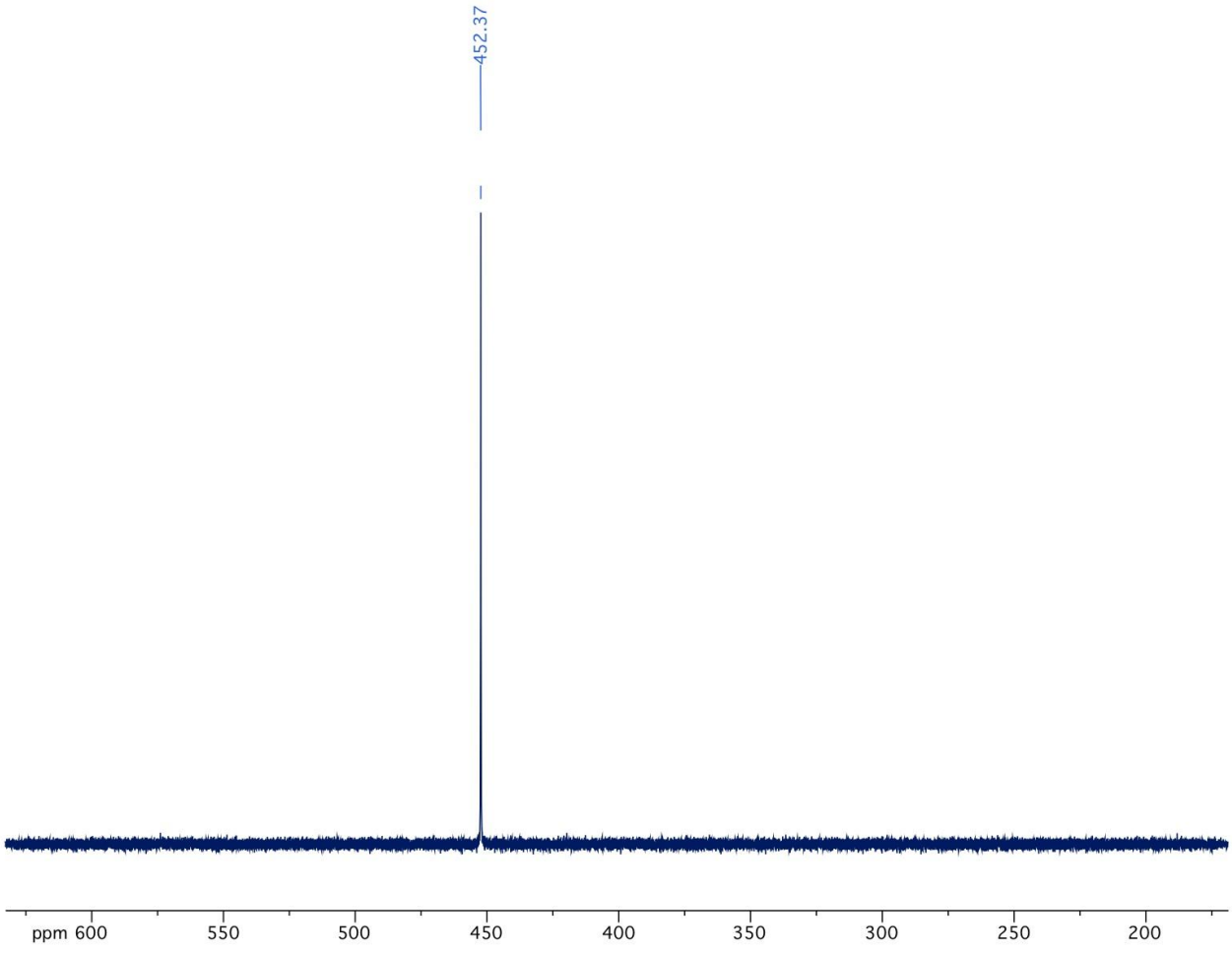

Figure S5. $^{31}P\{^{1}H\}$ NMR (C_6D_6, 161.97 MHz, 20 ^{o}C) spectrum of $(Ar[CMe_3CH_2]N)_3TaPPh$ (**1**).

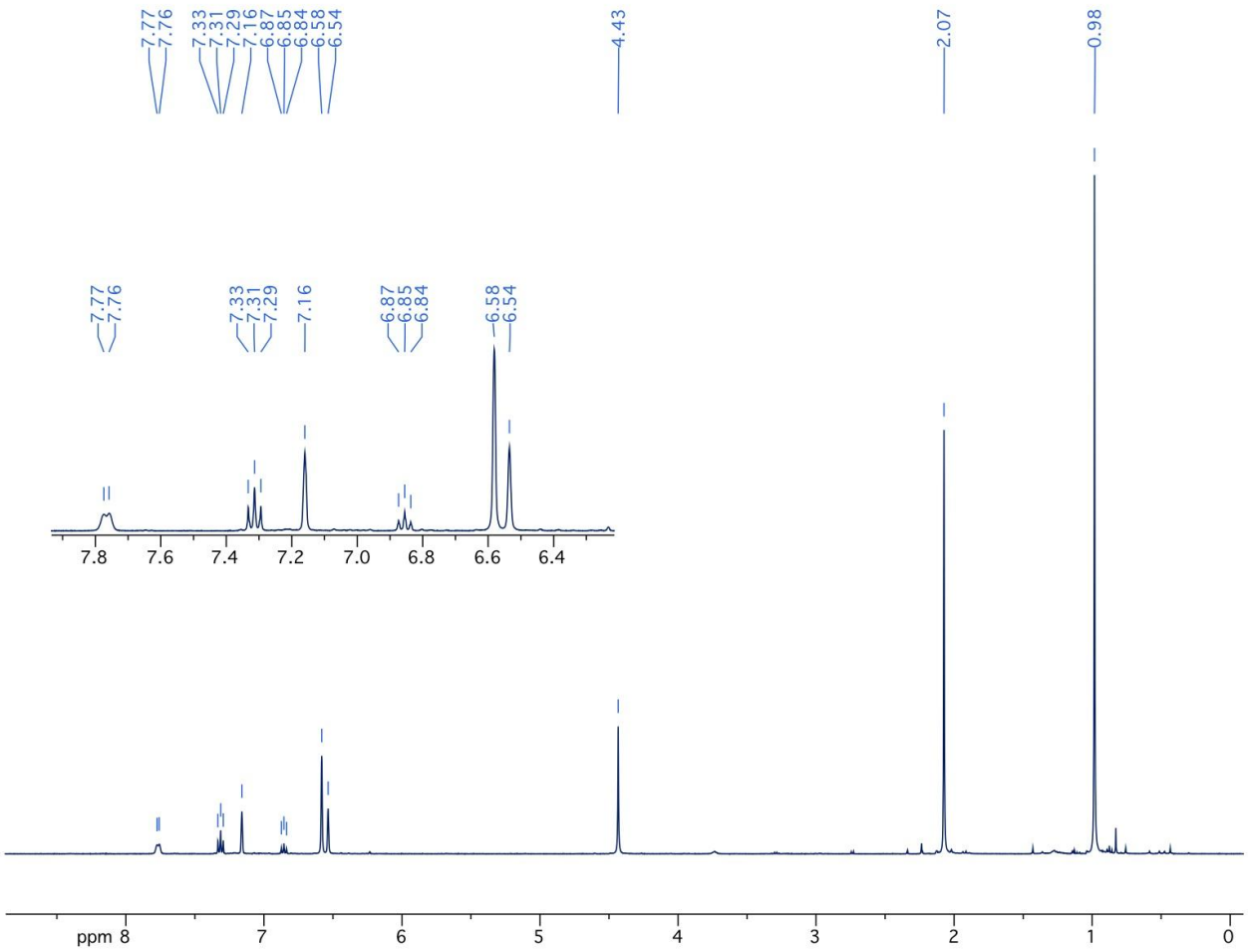

Figure S6. ^{1}H NMR (C_6D_6, 400.13 MHz, 20 ^{o}C) spectrum of ($Ar[CMe_3CH_2]N)_3TaPPh$ (**1**).

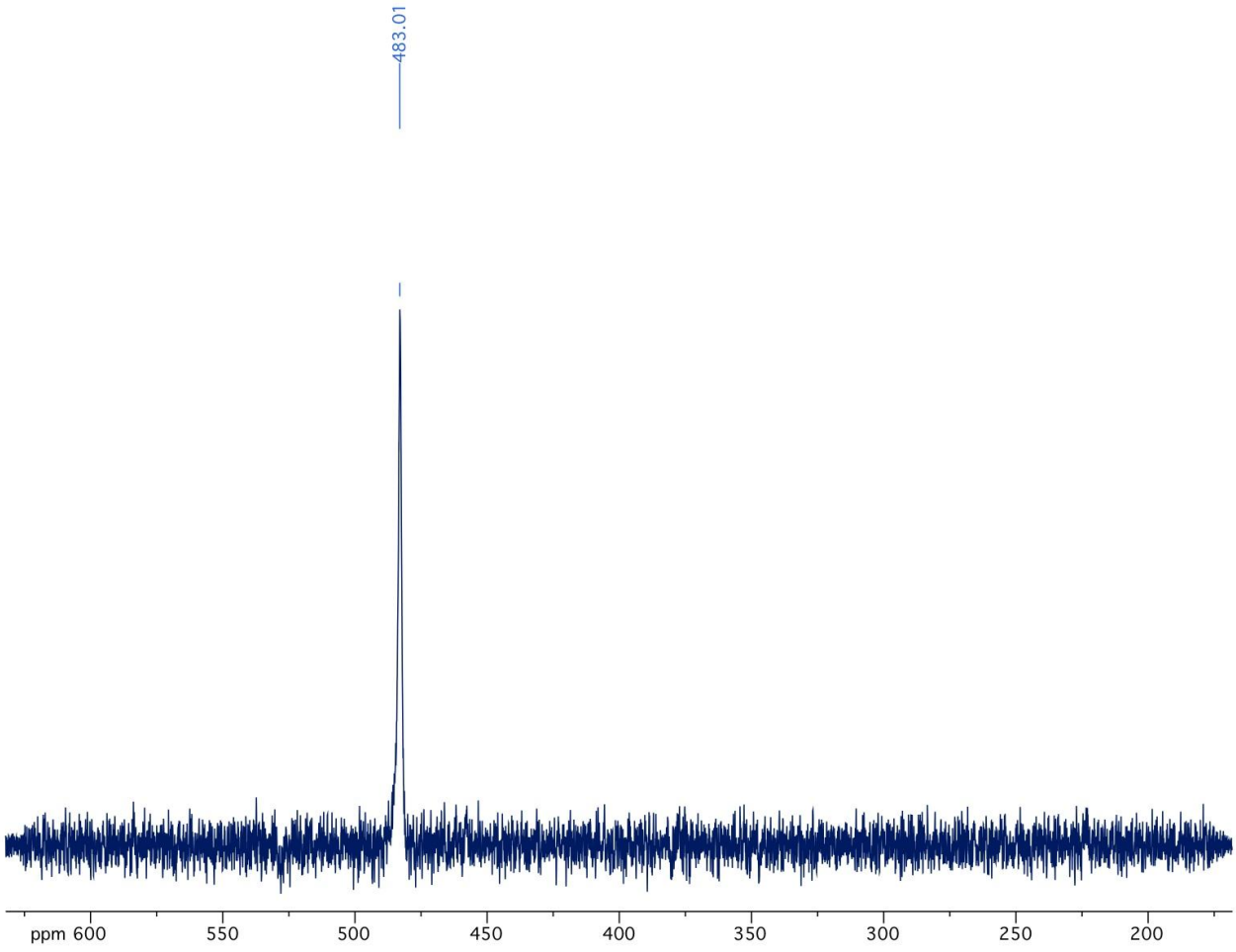

Figure S7. $^{31}P\{^{1}H\}$ NMR (C_6D_6, 161.97 MHz, 20 ^{o}C) spectrum of $(Ar[CMe_3CH_2]N)_3TaPCy$ (**6**).

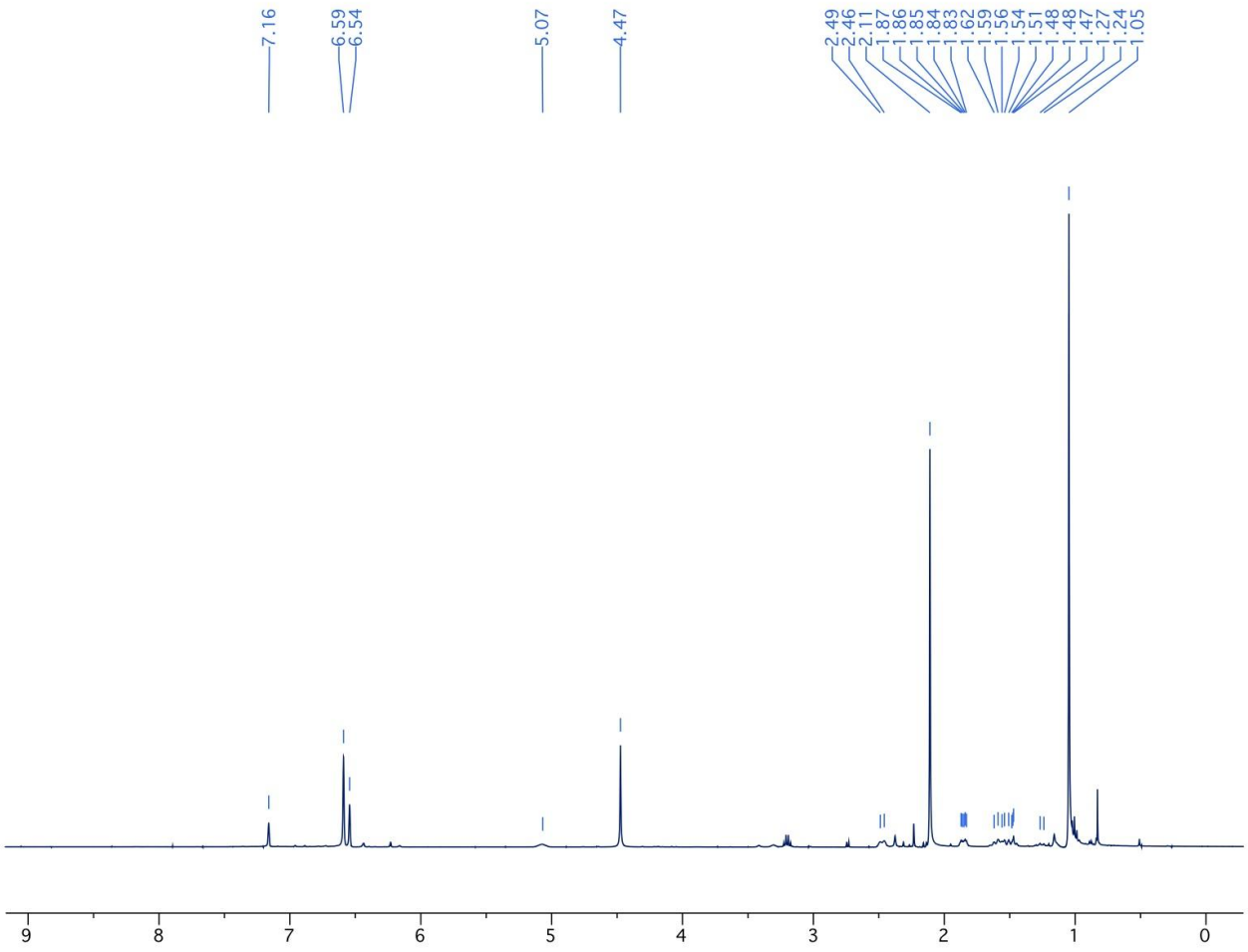

Figure S8. ^{1}H NMR (C_6D_6, 400.13 MHz, 20 ^{o}C) spectrum of (Ar[CMe_3CH_2]N)$_3$TaPCy (**6**). Resonances associated with minor amounts of Et_2O and unligated Ar[CMe_3CH_2]NH were left unmarked.[3,4]

SII. Crystallographic Structure Determinations

General Considerations. X-ray quality crystals were grown as described in the experimental procedures. Crystals were mounted in hydrocarbon oil on a nylon loop or a glass fiber. Low-temperature (100 K) data were collected on a Siemens Platform three-circle diffractometer coupled to a Bruker-AXS Smart Apex CCD detector with graphite-monochromated Mo Kα radiation (λ = 0.71073 Å) performing φ- and ω-scans. Software used for diffraction data processing and crystal structure solution and refinement are contained in the APEX2 v2008-3.0 program suite (Bruker AXS). A semi-empirical absorption correction was applied to the diffraction data using SADABS.[15] All structures were solved by direct or Patterson methods using SHELXS[16,17] and refined against F^2 on all data by full-matrix least squares with SHELXL-97.[17,18] In the case of $(Ar[CMe_3CH_2]N)_3TaPPh$ (**1**), the crystal used for data collection was found to display nonmerohedral twinning, and as such TWINABS was employed as the absorption correction method. Both components of the twin were indexed with the program CELL_NOW. Integrated intensities for the reflections from the two components were written into a SHELXL-93 HKLF 5 reflection file with the data integration program SAINT (version 7.53A), using all reflection data (exactly overlapped, partially overlapped, and non-overlapped). Two crystallographically independent molecules of $(Ar[CMe_3CH_2]N)_2(\eta^2$-$Me_3CC(H)NAr)TaP(H)Ph$ (**3**) were identified in the asymmetric unit, and were refined in a satisfactory manner; only one of the two independent molecules of **3** is depicted in the text. All non-hydrogen atoms were refined anisotropically. The hydrogen atoms attached to C17 in $(Ar[CMe_3CH_2]N)_2(\eta^2$-$Me_3CC(H)NAr)TaPPh_2$ (**5**), C17 and C47 in **3**, C41 in $(Ar[CMe_3CH_2]N)_3TaPCy$ (**6**), Ta in $[(Ar[CMe_3CH_2]N)_3TaH]_2$ (**8**), and C17 in $(Ar[CMe_3CH_2]N)_2(\eta^2$-$Me_3CC(H)NAr)TaCl$ (**4**) were located in the Fourier difference map and refined using appropriate distance restraints. Hydrogen atoms attached to phosphorous atoms in **3** could not be definitively identified in the Fourier difference map and thus were not included in the model. Complex **8** crystallizes in space group $R\bar{3}$ with one-sixth of the full molecule per asymmetric unit; in addition, there is a positional disorder of this moiety over two positions (fvar = 0.8247). Although we are hesitant to comment definitively regarding the bridging hydride positions in this structural determination given the associated amount of uncertainty, they were included in the model at probable locations for structural clarity. Supplemental support for the presence of bridging hydrides is described in the corresponding experimental section for **8**. Otherwise, hydrogen atoms were included in the model at geometrically calculated positions and refined using a riding model. The isotropic displacement parameters of all hydrogen atoms were fixed to 1.2 times the U_{eq} value of the atoms they are linked to (1.5 times for methyl groups). In structures where disorders were present the disorders were refined within SHELXL with the help of rigid bond restraints as well as similarity restraints on the anisotropic displacement parameters for neighboring atoms and on 1,2- and 1,3-distances throughout the disordered components.[19] The relative occupancies of disordered components were refined freely within SHELXL, while constraining the sum of the occupancies to unity. After location and refinement of atoms for $(Ar[CMe_3CH_2]N)_3TaCl_2$ (**9**), attempts to refine the remaining peaks of residual electron density as CH_2Cl_2 and $CHCl_3$ solvate molecules were unsuccessful. The data were corrected for disordered electron density through use of the SQUEEZE procedure,[20] as implemented in PLATON.[21] A total solvent-accessible void volume of 588 $Å^3$ with a total electron count of 192 (consistent with two molecules of $CHCl_3$ and two molecules of CH_2Cl_2 per asymmetric unit) was found in the unit cell. The .cif file was edited to contain all relevant SQUEEZE output. Further crystallographic data are given in Tables S1-S3. Complete crystallographic details are available in the form of Crystallographic Information Files (CIF). These data (CCDC 852392–852398) can be obtained free of charge from the Cambridge Crystallographic Data Centre via *www.ccdc.cam.ac.uk/data_request/cif*.

	5	**3**	**1**	**6**
CCDC no.	852398	852396	852392	852397
Empirical formula	$C_{51}H_{69}N_3PTa$	$C_{48.75}H_{73}N_3PTa$	$C_{45}H_{65}N_3PTa$	$C_{45}H_{71}N_3PTa$
Formula weight	936.01	913.02	859.92	865.97
Crystal dimensions	0.17 × 0.09 × 0.09	0.20 × 0.15 × 0.10	0.41 × 0.21 × 0.10	0.28 × 0.23 × 0.09
Crystal system	triclinic	triclinic	triclinic	triclinic
Space group	*P*-1	*P*-1	*P*-1	*P*-1
a (Å)	10.9124(7)	12.8823(8)	10.5963(16)	10.9320(12)
b (Å)	11.6952(7)	17.7431(12)	12.3639(19)	11.5291(12)
c (Å)	19.3712(12)	21.9477(15)	17.124(3)	18.468(2)
α (deg)	90.0170(10)	84.4240(10)	82.977(3)	102.234(2)
β (deg)	101.3980(10)	74.1600(10)	87.201(3)	91.533(2)
γ (deg)	103.3620(10)	87.8070(10)	74.186(3)	103.933(2)
V (Å^3)	2355.1(3)	4802.9(5)	2142.1(6)	2200.4(4)
Z	2	4	2	2
ρ_{calcd} (g cm^{-3})	1.320	1.263	1.333	1.307
μ (mm^{-1})	2.403	2.355	2.635	2.566
Range of transmission	0.8218–0.6855	0.7986–0.6502	0.7785–0.4113	0.8019–0.5335
2θ limit (deg)	60.06	56.44	58.26	60.94
	$-15 \le h \le 15$	$-17 \le h \le 16$	$-14 \le h \le 14$	$-15 \le h \le 15$
	$-16 \le k \le 16$	$-23 \le k \le 23$	$-16 \le k \le 16$	$-16 \le k \le 16$
	$-27 \le l \le 27$	$-29 \le l \le 29$	$0 \le l \le 23$	$-26 \le l \le 26$
Total data collected	51078	87774	11540	51261
Independent reflections	13630	23487	11540	13168
R_{int}	0.0433	0.0591	N/A	0.0509
Observed reflections	12042	17533	11283	11355
Data/restraints/parameters	13630 / 1 / 523	23487 / 114 / 1055	11540 / 0 / 467	13168 / 82 / 503
Goodness-of-fit	1.045	1.040	1.118	1.051
R_1 [$F_o^2 \ge 2\sigma(F_o^2)$]	0.0278	0.0399	0.0266	0.0329
wR_2 [$F_o^2 \ge -3\sigma(F_o^2)$]	0.0589	0.0814	0.0663	0.0655
Largest peak, hole (eÅ^{-3})	1.585, -0.945	2.785, -1.439	1.387, -1.158	1.449, -0.826

Table S1. Crystallographic Data for (Ar[CMe_3CH_2]N)$_2$(η^2-Me_3CC(H)*N*Ar)TaPPh$_2$ (**5**), (Ar[CMe_3CH_2]N)$_2$(η^2-Me_3CC(H)*N*Ar)TaP(H)Ph (**3**), (Ar[CMe_3CH_2]N)$_3$TaPPh (**1**), and (Ar[CMe_3CH_2]N)$_3$TaPCy (**6**).

	8	**9**	**4**
CCDC no.	852393	852394	852395
Empirical formula	$C_{78}H_{124}N_6Ta_2$	$C_{37.5}H_{61}Cl_{3.25}N_3Ta$	$C_{39}H_{59}N_3ClTa$
Formula weight	1507.70	874.08	786.29
Crystal dimensions	0.45 × 0.45 × 0.10	0.44 × 0.32 × 0.27	0.15 × 0.10 × 0.02
Crystal system	hexagonal	monoclinic	monoclinic
Space group	*R*-3	*C*2/*c*	$P2_1/c$
a (Å)	12.9616(9)	22.3929(19)	11.9313(16)
b (Å)	12.9616(9)	13.1868(11)	35.046(5)
c (Å)	38.840(3)	29.573(3)	9.5018(12)
α (deg)	90	90	90
β (deg)	90	108.0310(10)	106.182(2)
γ (deg)	120	90	90
V (Å^3)	5651.0(7)	8304.0(12)	3815.7(9)
Z	3	8	4
ρ_{calcd} (g cm^{-3})	1.329	1.398	1.369
μ (mm^{-1})	2.946	2.866	2.980
Range of transmission	0.7571–0.3507	0.5096–0.3633	0.9428–0.6635
2θ limit (deg)	60.06	59.14	59.14
	$-18 \le h \le 18$	$-31 \le h \le 30$	$-16 \le h \le 16$
	$-18 \le k \le 17$	$-18 \le k \le 18$	$-48 \le k \le 48$
	$-54 \le l \le 54$	$-41 \le l \le 41$	$-13 \le l \le 13$
Total data collected	36616	103293	85345
Independent reflections	3690	11619	10700
R_{int}	0.0375	0.0445	0.0747
Observed reflections	3490	10572	8801
Data/restraints/parameters	3690 / 384 / 255	11619 / 0 / 421	10700 / 1 / 415
Goodness-of-fit	1.105	1.067	1.084
R_1 [$F_o^2 \ge 2\sigma(F_o^2)$]	0.0215	0.0347	0.0334
wR_2 [$F_o^2 \ge -3\sigma(F_o^2)$]	0.0515	0.0855	0.0706
Largest peak, hole (eÅ^{-3})	1.277, -0.953	2.234, -0.764	1.513, -1.145

Table S2. Crystallographic Data for $[(Ar[CMe_3CH_2]N)_3TaH]_2$ (**8**), $(Ar[CMe_3CH_2]N)_3TaCl_2$ (**9**), and $(Ar[CMe_3CH_2]N)_2(\eta^2\text{-}Me_3CC(H)NAr)TaCl$ (**4**).

	5	**3**	**1**	**6**
Ta–P	2.5312(6)	2.5543(12)	2.3052(11)	2.2888(8)
Ta–C17	2.200(2)	2.222(4)		
Ta–N1	1.976(2)	1.966(3)	1.989(3)	1.994(2)
Ta–N2	1.9914(19)	1.970(3)	1.989(3)	1.979(2)
Ta–N3	1.9656(19)	1.966(3)	2.005(3)	2.021(2)
N1–C17	1.418(3)	1.427(5)	1.500(5)	1.498(4)
Ta–P–C	104.45(7), 112.01(7)	83.76(11)	125.15(13)	130.07(10)
N1–Ta–C17	39.25(8)	39.25(13)		
C17–N1–Ta	78.94(13)	80.1(2)	126.5(3)	127.22(19)

Table S3. Selected Interatomic Distances (Å) and Angles (deg) for **5**, **3**, **1**, and **6**.

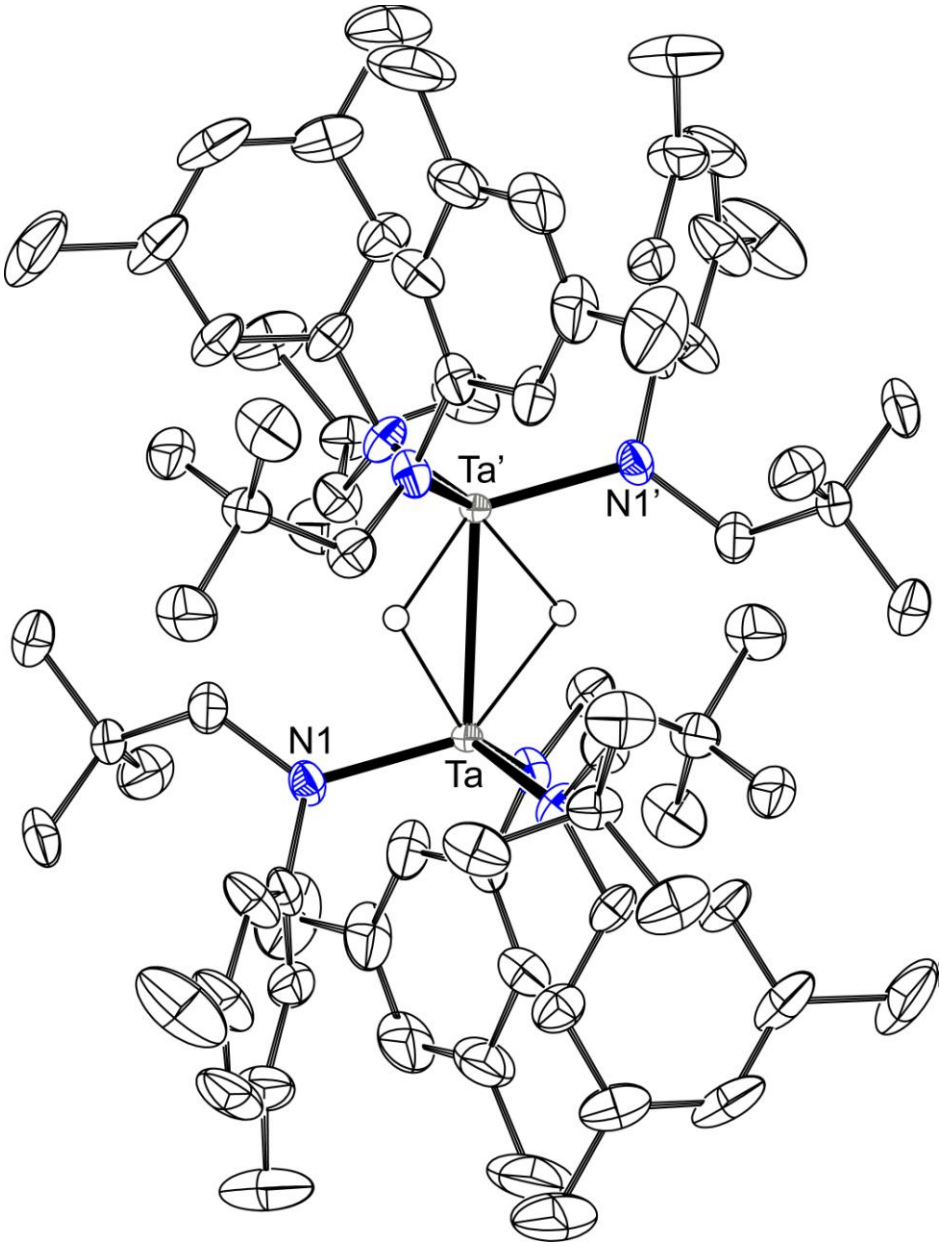

Figure S9. ORTEP rendering[21] of $[(Ar[CMe_3CH_2]N)_3TaH]_2$ (**8**) with thermal ellipsoids at 50% probability and selected H atoms omitted for clarity.

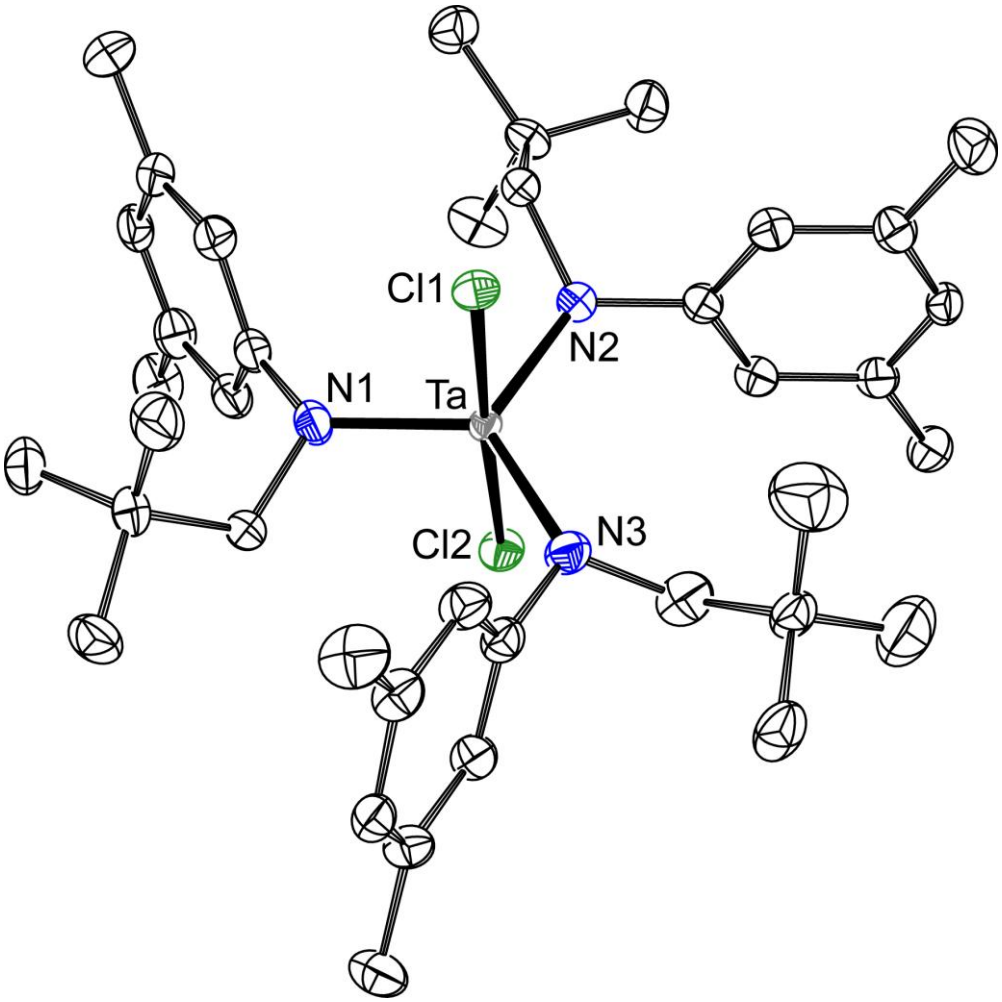

Figure S10. ORTEP rendering[21] of $(Ar[CMe_3CH_2]N)_3TaCl_2$ (**9**) with thermal ellipsoids at 50% probability and H atoms omitted for clarity.

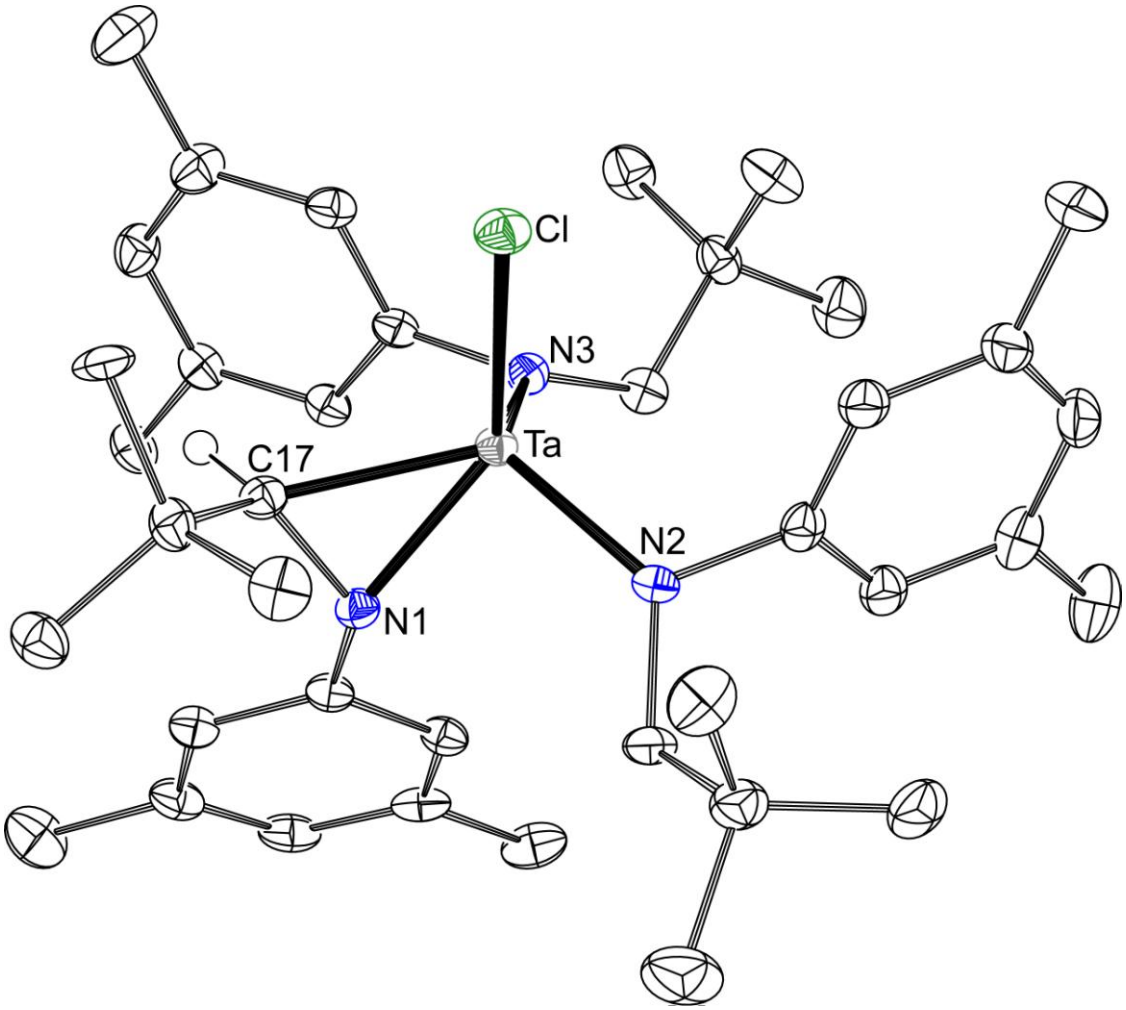

Figure S11. ORTEP rendering[21] of (Ar[CMe_3CH_2]N)$_2$(η^2-Me_3CC(H)*N*Ar)TaCl (**4**) with thermal ellipsoids at 50% probability and selected H atoms omitted for clarity.

SIII. References

1. Rankin, M. A.; Cummins, C. C. *J. Am. Chem. Soc.* **2010**, *132*, 10021.

2. Schlosser, M.; Hartmann, J. *Angew. Chem., Int. Ed. Engl*. **1973**, *12*, 508.

3. Fulmer, G. R.; Miller, A. J. M.; Sherden, N. H.; Gottlieb, H. E.; Nudelman, A.; Stoltz, B. M.; Bercaw, J. E.; Goldberg, K. I. *Organometallics* **2010**, *29*, 2176.

4. Figueroa, J. S.; Cummins, C. C. *J. Am. Chem. Soc.* **2003**, *125*, 4040.

5. For characterization data for $(^{t}Bu_3SiO)_3Ta(H)P(H)Ph$, see: (*a*) Bonanno, J. B.; Wolczanski, P. T.; Lobkovsky, E. B. *J. Am. Chem. Soc.* **1994**, *116*, 11159; (*b*) Hulley, E. B.; Bonanno, J. B.; Wolczanski, P. T.; Cundari, T. R.; Lobkovsky, E. B. *Inorg. Chem.* **2010**, *49*, 8524. For characterization data for $(^{t}Bu_3SiO)_3Ta(H)_2$, see: (*c*) Lapointe, R. E.; Wolczanski, P. T. *J. Am. Chem. Soc.* **1986**, *108*, 3535.

6. Structurally related complexes of the type $[X_3TaH]_2$ (X = monoanionic ligand) have been reported: (*a*) Belmonte, P. A.; Schrock, R. R.; Day, C. S. *J. Am. Chem. Soc.* **1982**, *104*, 3082; (*b*) Cotton, F. A.; Daniels, L. M.; Murillo, C. A.; Wang, X. *J. Am. Chem. Soc.* **1996**, *118*, 12449; (*c*) Chadeayne, A. R.; Wolczanski, P. T.; Lobkovsky, E. B. *Inorg. Chem.* **2004**, *43*, 3421.

7. The expected region for a terminal Ta−H absorbance is 1900 ± 300 cm^{-1}, see: (*a*) Kaesz, H. D.; Saillant, R. B. *Chem. Rev.* **1972**, *72*, 231. For references regarding IR absorbances of tantatum hydrides, see: (*b*) Fryzuk, M. D.; MacKay, B. A.; Patrick, B. O. *J. Am. Chem. Soc.* **2003**, *125*, 3234; (*c*) Gavenonis, J.; Tilley, T. D. *Organometallics* **2004**, *23*, 31; (*d*) Watanabe, T; Ishida, Y.; Matsuo, T.; Kawaguchi, H. *J. Am. Chem. Soc.* **2009**, *131*, 3474; (*e*) Ref. 1.

8. The related crystallographically determined structure of $(Ar[CMe_3CH_2]N)_3Nb(O_3SCF_3)_2$ has been reported: Figueroa, J. S.; Cummins, C. C. *J. Am. Chem. Soc.* **2004**, *126*, 13916.

9. Waterman, R.; Tilley, T. D. *Chem. Sci.* **2011**, *2*, 1320.

10. The Nb analog was prepared by a similar approach, see: (*a*) J. S. Figueroa, Ph.D. Thesis, Massachusetts Institute of Technology, 2005. For reports describing related cystallographically characterized tantalaziridine chloride complexes, see: (*b*) Scoles, L.; Ruppa, K. B. P.; Gambarotta, S. *J. Am. Chem. Soc.* **1996**, *118*, 2529; (*c*) Boncella, J. M.; Cajigal, M. L.; Abboud, K. A. *Organometallics* **1996**, *15*, 1905; (*d*) Takai, K.; Ishiyama, T.; Yasue, H.; Nobunaka, T.; Itoh, M.; Oshiki, T.; Mashima, K.; Tani, K. *Organometallics* **1998**, *17*, 5128; (*e*) Bazinet, P.; Yap, G. P. A.; Richeson, D. S. *Organometallics* **2001**, *20*, 4129; (*f*) Spencer, L. P.; Beddie, C.; Hall, M. B.; Fryzuk, M. D. *J. Am. Chem. Soc.* **2006**, *128*, 12531.

11. For examples of complexes with a terminal Ta−PPh_2 linkage, see: (*a*) Domaille, P. J.; Foxman, B. M.; McNeese, T. J.; Wreford, S. S. *J. Am. Chem. Soc.* **1980**, *102*, 4114; (*b*) Baker, R. T.; Calabrese, J. C.; Harlow, R. L.; Williams, I. D. *Organometallics* **1993**, *12*, 830; (*c*) Nikonov, G. I.; Kuzmina, L. G.; Mountford, P.; Lemenovskii, D. M. *Organometallics* **1995**, *14*, 3588; (*d*) Abdul Hadi, G. A.; Fromm, K.; Blaurock, S.; Jelonek, S.; Hey-Hawkins, E. *Polyhedron* **1997**, *16*, 721. Examples of Ta−PPh_2 linkages that bridge two metal centers are also known, see: (*e*) Poulard, C.; Boni, G.; Richard, P.; Moïse, C. *J. Chem. Soc., Dalton Trans.* **1999**, 2725; (*f*) Boni, G.; Blacque, O.; Sauvageot, P.; Poujaud, N.; Moïse, C.; Kubicki, M. M. *Polyhedron* 2002, *21*, 371; (*g*) Shaver, M. P.; Fryzuk, M. D. *Organometallics* **2005**, *24*, 1419; (*h*) Ref. 11d.

12. Although no examples of crystallographically characterized complexes featuring a terminal Ta−P(H)Ph linkage were found, related examples featuring other transition metals include: (*a*) Rocklage, S. M.; Schrock, R. R.; Churchill, M. R.; Wasserman, H. J. *Organometallics* **1982**, *1*, 1332; (*b*) Bohle, D. S.; Jones, T. C.; Rickard, C. E. F.; Roper, W. R. *J. Chem. Soc., Chem. Commun*. **1984**, 865; (*c*) Bohle, D. S.; Jones, T. C.; Rickard, C. E. F.; Roper, W. R. *Organometallics* **1986**, *5*, 1612; (*d*) Vaughn, G. A.; Hillhouse, G. L.; Rheingold, A. L. *Organometallics* **1989**, *8*, 1760; (*e*) Burn, M. J.; Fickes, M. G.; Hollander, F. J.; Bergman, R. G. *Organometallics* **1995**, *14*, 137; (*f*) Zanetti, N. C.; Schrock, R. R.; Davis, W. M. *Angew. Chem. Int. Ed. Engl.* **1995**, *34*, 2044; (*g*)

Mösch-Zanetti, N. C.; Schrock, R. R.; Davis, W. M.; Wanninger, K.; Seidel, S. W.; O'Donaghue, M. B. *J. Am. Chem. Soc.* **1997**, *119*, 11037; (*h*) Firth, A. V.; Stephan, D. W. *Inorg. Chem.* **1998**, *37*, 4732; (*i*) Roering, A. J.; MacMillan, S. N.; Tanski, J. M.; Waterman, R. *Inorg. Chem.* **2007**, *46*, 6855.

13. Cummins, C. C.; Schrock, R. R.; Davis, W. M. *Angew. Chem. Int. Ed. Engl.* **1993**, *32*, 756.

14. Byrm, M.; Jones, C.; Waugh, M.; Hey-Hawkins, E.; Majoumo, F. *New J. Chem.* **2003**, *27*, 1614.

15. Sheldrick, G. M. *SHELXTL*; Bruker AXS, Inc.: Madison, WI (USA), 2005–2008.

16. Sheldrick, G. M. *Acta Crystallogr.* **1990**, *A46*, 467.

17. Sheldrick, G. M. *Acta Crystallogr.* **2008**, *A64*, 112.

18. Sheldrick, G. M. *SHELXL-97: Program for crystal structure determination*; University of Göttingen, Göttingen, Germany, 1997.

19. Müller, P.; Herbst-Irmer, R.; Spek, A. L.; Schneider, T. R.; Sawaya, M. R. *Crystal Structure Refinement: A Crystallographer's Guide to SHELXL*; Müller, P., Ed.; IUCr Texts on Crystallography; Oxford University Press: Oxford, 2006.

20. van der Sluis, P.; Spek, A. L. *Acta Crystallogr.* **1990**, *A46*, 194.

21. Spek, A. L. *J. Appl. Cryst.* **2003**, *36*, 7.